



HAL
open science

A new semi-empirical model for the oxidation of PAHs physisorbed on soot. I. Application to the reaction $C_6H_6 + OH$.

Sylvain Picaud, Gyorgy Hantal, Barbara Collignon, Paul N.M. Hoang, Jean-Claude Rayez, Marie-Thérèse Rayez

► To cite this version:

Sylvain Picaud, Gyorgy Hantal, Barbara Collignon, Paul N.M. Hoang, Jean-Claude Rayez, et al.. A new semi-empirical model for the oxidation of PAHs physisorbed on soot. I. Application to the reaction $C_6H_6 + OH$. *Molecular Simulation*, 2009, 35 (12-13), pp.1130-1139. 10.1080/08927020902874016 . hal-00530450

HAL Id: hal-00530450

<https://hal.science/hal-00530450>

Submitted on 29 Oct 2010

HAL is a multi-disciplinary open access archive for the deposit and dissemination of scientific research documents, whether they are published or not. The documents may come from teaching and research institutions in France or abroad, or from public or private research centers.

L'archive ouverte pluridisciplinaire **HAL**, est destinée au dépôt et à la diffusion de documents scientifiques de niveau recherche, publiés ou non, émanant des établissements d'enseignement et de recherche français ou étrangers, des laboratoires publics ou privés.

**A new semi-empirical model for the oxidation of PAHs
physisorbed on soot. I.
Application to the reaction C₆H₆ + OH.**

Journal:	<i>Molecular Simulation/Journal of Experimental Nanoscience</i>
Manuscript ID:	GMOS-2009-0008.R1
Journal:	Molecular Simulation
Date Submitted by the Author:	24-Feb-2009
Complete List of Authors:	Picaud, Sylvain; Institut UTINAM - UMR CNRS 6213, Universite de Franche-Comte Hantal, Gyorgy; Laboratory of Interfaces and Nanosized Systems, Institute of Chemistry, ELTE University; Institut UTINAM - UMR CNRS 6213, Universite de Franche-Comte Collignon, Barbara; Institut UTINAM - UMR CNRS 6213, Universite de Franche-Comte Hoang, Paul N.M.; Institut UTINAM - UMR CNRS 6213, Universite de Franche-Comte Rayez, Jean-Claude; Institut des Sciences Moleculaires - UMR CNRS 5255, Universite de Bordeaux 1 Rayez, Marie-Thérèse; Institut des Sciences Moleculaires - UMR CNRS 5255, Universite de Bordeaux 1
Keywords:	semi-empirical method, soot, PAH , oxidation

1
2
3
4
5
6
7
8
9
10
11
12
13
14
15
16
17
18
19
20
21
22
23
24
25
26
27
28
29
30
31
32
33
34
35
36

A new semi-empirical model for the oxidation of PAHs physisorbed on soot. I. Application to the reaction $C_6H_6 + OH$.

37
38
39
40
41
42
43
44
45
46
47
48
49
50
51
52
53
54
55
56
57
58
59
60

G. Hantal,^{a,b} S. Picaud,^{a,*} B. Collignon,^a P.N.M. Hoang,^a
M.T. Rayez,^c J.C. Rayez^{c,*}

^a*Institut UTINAM - UMR CNRS 6213, Université de Franche-Comté, F-25030
Besançon Cedex, France*

^b*Laboratory of Interfaces and Nanosized Systems, Institute of Chemistry, Eötvös
Loránd University, Pázmány Péter stny. 1/a, H-1117 Budapest, Hungary.*

^c*Institut des Sciences Moléculaires - UMR CNRS 5255, Université de Bordeaux I,
F-33405 Talence Cedex, France*

Abstract

In the present paper, we have used a new semi-empirical method to characterize the oxidation by OH of a benzene molecule adsorbed on a soot surface modelled by a graphene-like cluster. This method is based on an electrostatic and induction contribution calculated at the SCF AM1 level associated with a sum of two-body dispersion terms of the $C^{(6)}/R^6$ form. This so-called AM1-D method has been used to compare the characteristics of the oxidation reaction for the adsorbed benzene with those of the corresponding reaction in the gas phase. The main conclusion of the present work is a clear inhibition of the oxidation process by the adsorption of the benzene molecule on the soot surface. This conclusion is in qualitative agreement with experimental observations, concerning however larger PAH molecules.

1
2
3 *Key words:* semi-empirical method, soot, PAH, oxidation
4
5
6
7
8
9
10
11
12
13
14
15
16
17
18
19
20
21
22
23
24
25
26
27
28
29
30
31
32
33
34
35
36
37
38
39
40
41
42
43
44
45
46
47
48
49
50

51 ^{_____}
52 * This paper is dedicated to the memory of our friend Jose Antonio Mejias who
53 initiated our work on soot surfaces.

54 * Corresponding authors.

55 *Email addresses:* sylvain.picaud@univ-fcomte.fr (S. Picaud),
56
57 jc.rayez@ism.u-bordeaux1.fr (J.C. Rayez).
58
59
60

1 Introduction

Polycyclic aromatic hydrocarbons (PAHs) are chemical pollutants ubiquitous in the atmosphere, aerosols, soils and sediments. They are mainly formed as by-products of combustion processes under oxygen-deficient conditions, and many of them and their degradation products are known or suspected allergen and carcinogens[1].

It has been long understood that the reactive fate of volatile PAHs (less than 3-4 rings) is governed by gas-phase reactions with the hydroxyl (OH) radical. However, due to their low vapor pressure and aromaticity, heavier PAHs are mostly adsorbed on fine carbonaceous particles[2] where they are subject of a wide range of heterogeneous chemical reactions depending on the particle composition[3–7]. This heterogeneous reactivity may thus be more important than the corresponding gas-phase reactions as sink for these compounds. Moreover, heterogeneous reactions of particle-bound PAHs may change the microphysical properties of the particle by making it more hygroscopic and hence modifying its cloud nucleation properties[8]. These heterogeneous reactions can also influence the atmospheric residence times of the carbonaceous particles and consequently their direct and indirect effects on climate[9,10].

During the incomplete combustion of carbonaceous fuels, PAHs are formed concurrently with soot particles and they play a significant role in soot formation and subsequent particle growth[11]. Soot is ubiquitous in the environment where it has been observed to comprise tens of percent of the total aerosol carbon in both rural and urban areas[12,13]. Because PAHs have a high affinity for carbonaceous materials, adsorption of PAHs on soot may be an important

1
2
3 mechanism affecting the gas-particle partitioning of PAHs[14].
4
5

6
7 Despite the importance of PAHs and soot particles interactions, their actual
8
9 effect on the radiative and chemical budgets of the atmosphere is still poorly
10
11 known and some of this uncertainty is due to the lack of knowledge about
12
13 the physicochemical properties of the soot substrate[15,16]. Fresh soot par-
14
15 ticles consist of spherical primary carbonaceous particles that aggregate into
16
17 larger clusters of fractal-like shape[17]. These primary particles are often made
18
19 of nanocrystallites containing graphite-type layers arranged in an onion-like
20
21 structure, with diameters ranging between 20 and 50 nm[18,19]. Soot particles
22
23 are usually associated with organic and inorganic soluble material at their sur-
24
25 faces. One of the major problem is thus that soot is not a well-defined chemical
26
27 substance[20]. Therefore, model particles are often used as a first approach to
28
29 study atmospheric chemical processes as they are simpler and better charac-
30
31 terized than natural particles[21,22]. There are several types of soot used for
32
33 laboratory studies of atmospheric effects: commercial soot[23], spark-discharge
34
35 soot[24,25], and soot resulting from the combustion of hydrocarbon fuels in
36
37 different burners[26,27]. However, different types of soot differ in particle size,
38
39 specific surface area, structure, and composition, and thus they may differ
40
41 in chemical properties. As a consequence, studies of the physico-chemistry of
42
43 PAHs on soot surfaces are very scarce. Up to now, there are only a limited
44
45 number of controlled laboratory[28,29] or field[30,31] studies on the adsorption
46
47 of gas-phase PAHs onto soot, and, to our best knowledge, there is only one
48
49 paper devoted to the experimental study of the uptake of aromatic hydrocar-
50
51 bons onto soot with a known surface area, as a function of temperature and
52
53 partial pressure[4].
54
55

56
57
58 In a recent study, Esteve et al.[21] have characterized the role of OH, NO₂
59
60

1
2
3 and NO radicals on the reactivity of 11 polyaromatic compounds adsorbed on
4 graphite particles chosen as a model of atmospheric carbonaceous particles.
5
6
7 The results showed that the reaction of particulate-PAHs with NO is negligible
8 under atmospheric conditions, whereas in the case of the NO₂ reaction, sig-
9 nificant differences in the reactivities have been observed. Moreover, all PAHs
10 present similar rate constants while reacting with OH, and, compared to the
11 reactivity in the gas phase, the heterogeneous reaction with OH radicals seems
12 to show a potential inhibiting effect of the graphite surface, meaning that the
13 mechanisms may be sensibly different[21].
14
15
16
17
18
19
20
21
22

23 From a theoretical point of view, structural and energetic information on the
24 interaction between PAHs and carbonaceous surfaces like soot is also very
25 scarce, primarily due to the fact that these systems are too large for tractable
26 *ab initio* calculations. Indeed, a theoretical realistic simulation of intermolec-
27 ular forces requires high level electronic quantum calculations to account for
28 dispersion effects. The expression "high level quantum calculations" means
29 the use of very large basis sets and a precise description of the correlation
30 energy. Even for a simple perturbative approach, double excitations on two
31 interacting molecules are necessary to mimic (in general rather poorly) disper-
32 sion effects. Then, the most accurate methods for determining the geometry
33 and binding energy of PAHs clusters are correlated quantum chemistry cal-
34 culations that use very large correlation-consistent basis sets. Moreover, very
35 large basis sets are necessary to minimize both the basis set convergence error
36 and the basis set superposition error (BSSE). Such high-level calculations re-
37 quire a great amount of computational resources[32] and if they are possible
38 for, i.e., benzene dimers[33], they are not conceivable for larger systems.
39
40
41
42
43
44
45
46
47
48
49
50
51
52
53
54
55

56 Recently, an interesting method - the Hartree-Fock Dispersion model (HFD)
57
58
59
60

1
2
3 - has been introduced by Gonzalez et al.[34,35] to calculate the structure and
4 binding energy of aromatic clusters, following the work originally proposed by
5 Hepburn et al.[36]. In this HFD method, the calculation of the intermolecular
6 energies combines an *ab initio* self-consistent field (SCF) interaction energy
7 with an empirical dispersion energy from the London theory, i.e., an analytical
8 approach much more efficient to describe dispersion than the direct calculation
9 from electronic correlation effects[34]. The accuracy of this method has been
10 tested in computing the equilibrium geometries and the binding energies of the
11 van der Waals dimers of benzene, naphthalene, anthracene, and pyrene, as well
12 as those of the naphthalene trimer[35]. However, even the HFD method is pro-
13 hibited for a theoretical characterization of the PAHs/soot interactions, when
14 considering large size PAHs and/or large graphite clusters modelling the soot
15 surface. We have thus introduced, in a recent paper[37], a new method where
16 the SCF calculations are performed at a semi-empirical level by including ex-
17 plicitly the valence electrons only. This method, so called the SE-D method,
18 combines the semi-empirical description of the electrostatic and induction in-
19 teractions to a sum of two-body London dispersion terms of the $C^{(6)}/R^6$ form.
20 The empirical parameters of this method have been fitted on a set of *ab initio*
21 and experimental results for 22 PAHs dimers and mixed complexes, aiming
22 at defining a transferable interaction potential for the calculations of disper-
23 sion energy between aromatic molecules and large graphite clusters[37]. Three
24 sets of transferable parameters have thus been determined for combination
25 with electrostatic and induction interactions performed at the AM1, PM3, or
26 MNDO level of theory, with, however, slightly better results when the disper-
27 sion parameters are combined with the AM1 and PM3 methods than with the
28 MNDO method[37,38].
29
30
31
32
33
34
35
36
37
38
39
40
41
42
43
44
45
46
47
48
49
50
51
52
53
54
55
56
57
58
59
60

1
2
3 It is worth mentioning that such an approach that aims at describ-
4 ing intermolecular interactions in large carbonaceous systems on the
5 basis of semi-empirical calculations shows similarities with meth-
6 ods recently developed to improve the semi-empirical description
7 of other systems for which refined quantum calculations are too
8 costly. For example, electrostatic and dispersion corrections have
9 been brought to the AM1 or PM3 semi-empirical energy to repro-
10 duce correctly the long-range behavior of the interaction potential
11 in hydrogen bonded systems[39–41]. Similarly, an atom-atom pair-
12 wise additive dispersion potential has also been recently added to
13 a semi-empirical description of the intermolecular interactions in
14 biomolecules[42].
15
16
17
18
19
20
21
22
23
24
25
26
27
28
29
30
31
32
33
34
35
36
37
38

39 In the present paper, we make use of the SE-D method to characterize the ox-
40 idation mechanisms of PAH molecules adsorbed at the soot surface modelled
41 by a large carbon cluster of graphene type. Such a large cluster has been pre-
42 viously used to model soot surfaces interacting with water molecules using *ab*
43 *initio* approaches[43–45]. The theoretical backgrounds of our study are given
44 in Section 2, and, as a first application, the results of the detailed investigation
45 of the heterogeneous oxidation reaction of benzene adsorbed on soot are then
46 presented in Section 3. These results are compared with those obtained in the
47 gas phase and they are discussed on the basis of experimental observations in
48 Section 4.
49
50
51
52
53
54
55
56
57
58
59
60

2 Theoretical backgrounds

2.1 The SE-D method

In this section, we briefly recall the main basis of the SE-D model[37,38]. In this model, a dispersion term (U_D) is added to a semi-empirical determination of the electrostatic and induction interactions to account for dispersion forces in the calculation of the total energy. This total energy for a PAH adsorbed on a carbonaceous particle modelling a soot surface is thus written as

$$U_{\text{SE-D}} = U_{\text{SE}} + f \times U_D, \quad (1)$$

where U_{SE} is the semi-empirical energy calculated at the AM1, PM3, or MNDO level of theory, U_D is the dispersion energy, and f is a damping function used to avoid singularities in the dispersion term at short intermolecular distances. Note that these semi-empirical methods are proposed to reproduce, within an given average accuracy, geometries, heats of formation and some other thermodynamical data. These quantities are mainly due to "chemical forces" which are responsible for bond energies i.e. energy differences between separated fragments and the interacting systems at equilibrium distances. However, due to the reduced basis set used (valence atomic orbitals), it is impossible to reproduce a long range quantum effect like dispersion. It is already almost impossible to do it with a "reasonably good" *ab initio* approach. On the contrary, long range electrostatic and induction effects, which are not at all quantum in nature but strictly classical, are included in a

more or less realistic way in the calculations by the self-consistent field procedure itself. The electrostatic interaction energy is given by the first SCF iteration and the induction energy at the SCF convergence since the electronic cloud, which corresponds to the average electronic field felt by each electron, reaches its final shape at the end of the SCF iterations. It turns out that the introduction of a sum of $-R^{-6}$ terms added at long distance to the SCF energy appears as an elegant way to include dispersion, even if it requires some "savoir-faire" for the estimation of these terms.

The dispersion contribution to the total energy is thus expressed as[46]

$$f \times U_D = - \sum_{i=1}^{N_g} \sum_{j=1}^{N_p} \frac{1}{(1 + e^{\alpha(R_0 - R_{ij})})} \times \frac{[C_i^{(6)} C_j^{(6)}]^{1/2}}{R_{ij}^6}, \quad (2)$$

where N_g and N_p are the total number of atoms on the carbonaceous surface and in the PAH molecule considered, respectively. R_{ij} is the interatomic distance between a surface atom i and the j th atom of the PAH molecule, and $C^{(6)}$ represents the two-body dispersion coefficients used to calculate the C-C, C-H and H-H interactions. The damping function $f(R_{ij})$ has the two-parameter hyperbolic tangent function form proposed by Gonzales et al.[34,35], in which α and R_0 are two empirical parameters that monitor the behavior of the damping function, and thus of the dispersion interaction, as a function of the interatomic distances R_{ij} .

The dispersion parameters α , R_0 , and $C_j^{(6)}$ of the SE-D approach have been fitted for the combination with a semi-empirical calculation of the SCF contribution to the interaction energy. These parameters have been proved to be

transferable from one PAH to another one[37,38]. Here, we choose the SE-D set of parameters suitable for use with the semi-empirical AM1 method because it has proven to give slightly more reliable results than the set of parameters suitable for use with the PM3 and MNDO methods (see Ref. [37]). However, the present study is not limited to the calculation of the interaction between PAHs and soot surface because it aims also at characterizing the oxidation of the adsorbed PAHs by the OH radical. We thus extend here the SE-D method to the calculations of the OH-PAH and OH-soot interactions, which are then written as

$$U_{\text{AM1-D}}^{\text{OH}} = U_{\text{AM1}}^{\text{OH}} - \sum_{i=1}^N \frac{1}{(1 + e^{\alpha^{\text{OH}}(R_0^{\text{OH}} - R_{i\text{O}})})} \times \frac{[C_{\text{O},i}^{(6)}]}{R_{i\text{O}}^6}, \quad (3)$$

where the semi-empirical calculations are performed at the AM1 level for the consistency with the calculations of the PAH-soot interactions. The sum over i includes the total number N of carbon atoms in the system considered (soot +PAH), and the $C_{\text{O},i}^{(6)}$ parameter for the oxygen-carbon interactions is taken from the literature[47]. Note that all the hydrogen atoms are neglected in the calculations of the OH-soot and OH-PAH interactions. **This assumption is based on the very weak contribution of these terms to the dispersion interactions in water-carbonaceous systems [48,49].** Determining the best values for the α^{OH} and R_0^{OH} parameters of the damping function is a delicate task which will be detailed below. All the parameters used in the present calculations are given in Table 1.

2.2 Energetics of the oxidation reaction

The mechanism of the oxidation reaction of PAH molecules by the OH radical is illustrated by the reaction scheme given in Figure 1.

In the first step of the reaction, a complex is formed between the reactants (the so-called pre-reactive complex, PRC) that, in the second step, transforms to the transition state (TS). Finally, the reaction results in the product that contains an sp^3 carbon atom and a π electron system with one missing electron. Defining the energies with respect to a reference state corresponding to the reactants far from each other, the PRC is located in an energy well (i.e., it corresponds to the negative energy E_1) while the TS corresponds to an energy barrier ($E_1 - E_2$) along the reaction path. Such a transition state formed with OH radical was found both theoretically and experimentally in the case of hydrocarbons[50], and aromatic hydrocarbons such as benzene[51–53], toluene[54] and phenol[55].

2.3 Kinetics of the oxidation reaction

The kinetics of the oxidation mechanism presented in Fig. 1 is governed by rate constants corresponding to the separate elementary reaction steps. The two first steps, schematized as



correspond to the formation of the PRC, characterized by the rate constant k_1 , and to the decay of the PRC to the reactants, governed by the rate con-

stant k_{-1} . Then, the formation of the product through the transition state is characterized by the rate constant k_2 as



Finally, it should be taken into account that the PRC can be quenched by collisions with neutral particles as,



This quenching step is characterized by the second order rate constant k_3 and M can be any neutral particle that does not experience any chemical transformation during the collision.

Then the global reaction rate for the oxidation process (i.e., the reaction rate for the formation of the product from the reactants) can be written in the following form:

$$r = \frac{d[\text{Product}]}{dt} = k_2[\text{PRC}] = k[\text{OH}][\text{PAH}]. \quad (7)$$

If we assume now that the PRC is in a quasi-steady state, then we arrive at the following expression for the total rate constant

$$k = \frac{k_1 k_2}{k_{-1} + k_2 + k_3[\text{M}]}. \quad (8)$$

We can make now two additional assumptions. First, we consider the existence of an equilibrium between the reactants and the PRC, such that the decay of

1
2
3 the PRC to reactants is much faster than the formation of the product, i.e.,
4
5
6
7

$$8 \quad k_{-1} \gg k_2. \quad (9)$$

10
11 Moreover, under tropospheric conditions, the pressure is low enough so that
12 the collisions with neutral particles are considerably rare events. We can thus
13 assume that
14
15
16
17

$$18 \quad k_2 \gg k_3[M]. \quad (10)$$

19
20 Finally, for the total rate constant, we obtain
21
22
23
24

$$25 \quad k = k_2 \frac{k_1}{k_{-1}} = k_2 K, \quad (11)$$

26
27 where K is the equilibrium constant of the formation of the PRC. Note that we
28 arrive at an expression similar to the one proposed by Atkinson and Cvetanovic
29 for the characterization of the addition of O atoms to olefins[56].
30
31
32
33

34 2.4 Calculations of K and k_2

35
36 The canonical equilibrium constant K for a gas-phase process is given by
37
38
39
40
41
42

$$43 \quad K = \frac{Q_{PRC}}{Q_{PAH}Q_{OH}} e^{-E_1/k_B T}, \quad (12)$$

44
45 where E_1 is the energy of the PRC with respect to the reference state (PAH
46 + OH at an infinite distance from each other), T is the absolute temperature,
47
48
49
50
51
52
53
54
55
56
57
58
59
60

k_B is the Boltzmann constant, and Q_{PRC} , Q_{PAH} and Q_{OH} are the partition functions of the pre-reactive complex, the polycyclic aromatic hydrocarbon and the OH radical, respectively.

The reaction constant for the formation of the product according to the transition state (TST) theory is expressed as

$$k_2 = \frac{k_B T}{h} \frac{Q^\ddagger}{Q_{PRC}} e^{-(E_2 - E_1)/k_B T}, \quad (13)$$

where h is the Planck constant, E_2 is the energy of the transition state with respect to the reference state and Q^\ddagger is the partition function of the transition state. According to Equation 11, the product of Equations 12 and 13 gives the total rate constant k

$$k = \frac{k_B T}{h} \frac{Q^\ddagger}{Q_{PAH} Q_{OH}} e^{-E_2/k_B T}, \quad (14)$$

expression in which E_1 no longer appears.

Because we are interested here in the modification of the rate constant k upon physisorption of the PAH on a carbonaceous particle modelling a soot surface, we rather choose to evaluate the ratio of the total rate constant of the oxidation in the gas phase to the one associated with the oxidation in the adsorbed phase, as

$$\frac{k^{ads}}{k^{gas}} = \frac{Q_{PAH}^{gas} Q_{OH}^{gas} Q^{\ddagger,ads}}{Q_{PAH}^{ads} Q_{OH}^{ads} Q^{\ddagger,gas}} e^{\frac{-(E_2^{ads} - E_2^{gas})}{k_B T}}. \quad (15)$$

3 Results and discussion

As a first application, we investigate here the details of the heterogeneous oxidation reaction of benzene adsorbed on a soot particle modelled by a large cluster of 80 carbon atoms arranged in fused benzene rings as in a graphene sheet. Note that, as in our previous studies[43–45], the dangling bonds of this cluster have been saturated with hydrogen atoms, and the cluster will thus be referred below as the $C_{80}H_{22}$ cluster. For these adsorbed species, the calculations have been performed with the AM1-D method.

3.1 Determination of the α and R_0 parameters for O-C interactions

First, we have determined the values of the α^{OH} and R_0^{OH} parameters of the damping function used for the calculations of the dispersion contributions to the AM1-D method (see Equation 3) in the following way. We performed AM1 calculations to characterize the PRC and the TS corresponding to the oxidation reactions of benzene by OH in the gas phase. The results, given in Table 2, show that the equilibrium distance for the PRC is larger than 3.0 Å, and that the equilibrium distance for the corresponding TS is equal to 2.08 Å. To set up our SE-D model, we can thus reasonably think that the dispersion interactions between the incoming OH and the reacting benzene molecule play a significant role above 3.0 Å only, and should vanish between 2.1 and 3.0 Å. This leads us to choose a R_0 value equal to 2.75 Å for the O–C interactions in the OH–benzene system. The corresponding value of the α parameter has been chosen accordingly to ensure a smooth removing of the dispersion interactions between 2.0 and 3.0 Å [38]. Note that the R_0 values

1
2
3 defined here are in agreement with values previously fitted in the literature
4 on the basis of DFT calculations[52]. Note also that we will assume in the
5 following that the parameters selected here for the O–C dispersion interactions
6 are transferable to the calculations of the interactions between OH and soot.
7
8
9

10 11 12 13 14 15 *3.2 Analysis of the OH+PAH energy profile*

16
17
18 Here, we present the optimized geometries and adsorption energies of the PRC
19 and TS corresponding to the oxidation of benzene by OH when the benzene
20 molecule is adsorbed on the surface of a C₈₀H₂₂ cluster. Note that we have
21 considered only the situation in which the OH radical comes from the gas
22 phase even for the reaction taking place in the adsorbed phase (i.e., the OH
23 radical arrives perpendicularly to the cluster surface). Indeed, preliminary
24 calculations have shown that the OH radical is captured by the cluster when
25 arriving parallel to its surface, such as the oxidation reaction cannot take
26 place[38]. Moreover, the results obtained for the adsorbed species have also
27 been compared with the results of the same kind of calculations performed on
28 gas phase systems with both AM1 and AM1-D methods.
29
30
31
32
33
34
35
36
37
38
39
40
41

42
43 As an illustration of the obtained results, the optimized geometries of the
44 PRC and TS are given in Fig. 2 for the benzene+OH system adsorbed on the
45 C₈₀H₂₂ cluster. This figure shows that the OH radical approaches the ben-
46 zene molecule along a direction perpendicular to a C–C bond, in a symmetric
47 position with respect to the two C atoms. This PRC geometry is also found
48 when performing the optimization for the gas phase system using both AM1-
49 D and AM1(i.e., without the dispersion contribution) methods. Upon further
50 approach, OH slightly rotates and deviates from its symmetric position, such
51
52
53
54
55
56
57
58
59
60

1
2
3 as the optimized TS geometry corresponds to the attachment of OH directly
4 on one C atom of the benzene molecule. Similar features are calculated both
5 for the gas phase and for the adsorbed phase systems, using both AM1 and
6 AM1-D methods. Note that these geometries are very similar to those ob-
7 tained from DFT calculations characterizing the oxidation reaction in the gas
8 phase[52].
9

10
11
12
13
14
15
16
17 The energy values corresponding to these optimized geometries are given in
18 Table 2 together with the O–C (nearest C atom) distances. First, the values
19 given in Table 2 show that the energy values obtained with the method AM1-D
20 **are algebraically lower than the corresponding AM1 values without**
21 **any dispersion contribution. This result is not surprising since dis-**
22 **persions is an attractive interaction. Also, for the same reason, the**
23 **O–C distances are shorter when using the AM1-D method, but only**
24 **for the PRC**, showing the greater influence of the dispersion interactions on
25 the PRC than on the TS geometries due to the damping function. Further-
26 more, **the energy values obtained for the adsorbed systems (with the**
27 **AM1-D method) are algebraically lower than the energy values cal-**
28 **culated for the corresponding systems in gas phase with the same method,**
29 as a consequence of the attractive interaction between the adsorbed system
30 and the soot surface which thus tends to stabilize the different steps of the
31 oxidation reaction.
32
33
34
35
36
37
38
39
40
41
42
43
44
45
46
47
48
49
50

51 *3.3 Kinetics of the oxidation reaction : ratio of the rate constants*

52
53
54

55
56 Before calculating the different partition functions in Equation 15, we have
57 characterized separately the various motions of the benzene molecule and of
58
59
60

1
2
3 the TS complex in the gas phase and on the soot surface.
4
5

6
7 As an illustration of the corresponding results, we give in Fig. 3 the energy
8
9 curves obtained upon rotating the adsorbed benzene molecule around the z
10
11 axis, perpendicular to the surface of the $C_{80}H_{22}$ cluster (Fig. 3a) and around
12
13 the x axis parallel to this surface (Fig. 3b). The energy barriers for the rota-
14
15 tional motion around the z axis (Fig. 3a) are three times smaller than the $k_B T$
16
17 value at room temperature, and, as a consequence this rotational motion can
18
19 be considered as a free rotation in our calculations. In a similar way, Fig. 3b
20
21 shows that the energy variations upon slightly tilting the admolecule around
22
23 the x axis can be easily represented by considering the admolecule as a 1D
24
25 harmonic oscillator. In fact, this detailed study shows that all the various mo-
26
27 tions of the adsorbed benzene molecule and TS can be described, in a first
28
29 approach, either by free motions as in gas phase or by the rigid rotor and
30
31 harmonic oscillator approximations. This leads to the following assumptions :
32
33

34
35 - the translational partition functions in the directions which are parallel to the
36
37 $C_{80}H_{22}$ cluster surface (direction x and y) are the same in the adsorbed phase
38
39 and in the gas phase, due to the very weak interaction potential corrugation
40
41 of the cluster surface,
42
43

44
45 - for the same reason, the rotation around the z direction in the adsorbed
46
47 phase can be approximated by a free rotor.
48
49

50
51 - by contrast, the translation in the z direction (i.e. perpendicular to the
52
53 surface) as well as the rotations around the x and y axes are hindered due
54
55 to the presence of the cluster surface and have to be treated as vibrational
56
57 motions.
58
59
60

Moreover, on the basis of the energy calculations presented above, we can use the following additional approximations to calculate the ratio k^{ads}/k^{gas} :

- the OH radical can be considered as in gas phase, even if the reaction takes place in the adsorbed phase. This assumption is justified by the fact that an OH radical approaching the graphene sheet could be captured such as **the oxidation reaction cannot occur**[38]. Moreover, the OH radical approaches toward the PAH only from the gas phase above the PAH plane.

- the internal vibrational modes and the electronic states are the same in the adsorbed phase and in the gas phase for the benzene molecule and for the TS, because of the weak interaction with the soot surface characterizing a physisorption process.

Using these assumptions, it turns out that the partition function ratios become

$$\frac{Q_{PAH}^{gas}}{Q_{PAH}^{ads}} = \frac{Q_{trans,z}^{gas,PAH}}{Q_{tr_z \rightarrow vibr}^{ads,PAH}} \frac{Q_{rot}^{gas,PAH}}{Q_{rot_x \rightarrow vibr}^{ads,PAH} Q_{rot_y \rightarrow vibr}^{ads,PAH} Q_{rot_z}^{ads,PAH}}, \quad (16)$$

and

$$\frac{Q_{tr_z \rightarrow vibr}^{\ddagger,ads}}{Q_{tr_z \rightarrow vibr}^{\ddagger,gas}} = \frac{Q_{tr_z \rightarrow vibr}^{\ddagger,ads}}{Q_{trans,z}^{\ddagger,gas}} \frac{Q_{rot_x \rightarrow vibr}^{\ddagger,ads}}{Q_{rot_x \rightarrow vibr}^{\ddagger,gas}} \frac{Q_{rot_y \rightarrow vibr}^{\ddagger,ads}}{Q_{rot_y \rightarrow vibr}^{\ddagger,gas}} \frac{Q_{rot_z}^{\ddagger,ads}}{Q_{rot_z}^{\ddagger,gas}}. \quad (17)$$

Finally, reporting the above equations into Equation 15, we arrive at the following expression of the rate constants ratio,

$$\begin{aligned} \frac{k^{ads}}{k^{gas}} &= \frac{Q_{trans,z}^{gas,PAH}}{Q_{tr_z \rightarrow vibr}^{ads,PAH}} \frac{Q_{rot}^{gas,PAH}}{Q_{rot_x \rightarrow vibr}^{ads,PAH} Q_{rot_y \rightarrow vibr}^{ads,PAH} Q_{rot_z}^{ads,PAH}} \\ &\times \frac{Q_{tr_z \rightarrow vibr}^{\ddagger,ads}}{Q_{tr_z \rightarrow vibr}^{\ddagger,gas}} \frac{Q_{rot_x \rightarrow vibr}^{\ddagger,ads}}{Q_{rot_x \rightarrow vibr}^{\ddagger,gas}} \frac{Q_{rot_y \rightarrow vibr}^{\ddagger,ads}}{Q_{rot_y \rightarrow vibr}^{\ddagger,gas}} \frac{Q_{rot_z}^{\ddagger,ads}}{Q_{rot_z}^{\ddagger,gas}} e^{\frac{-(E_2^{ads} - E_2^{gas})}{k_B T}}. \end{aligned} \quad (18)$$

where the following analytical expressions, valid for 1D and 3D rotations, 1D translation and 1D harmonic vibration, respectively, can be used for the calculations of the partition functions:

$$Q_{transl}^{1D} = L \sqrt{\frac{mk_B T}{2\pi\hbar^2}}, \quad (19)$$

$$Q_{vibr} = \frac{1}{1 - e^{-\frac{h\nu}{k_B T}}}, \quad (20)$$

$$Q_{rot}^{1D} = \frac{1}{\sigma} \sqrt{\frac{8\pi k_B T}{\hbar^2}} I, \quad (21)$$

$$Q_{rot}^{3D} = \frac{8\pi^2}{\sigma} \left(\frac{k_B T}{2\pi\hbar^2} \right)^{\frac{3}{2}} \sqrt{I_1 I_2 I_3}. \quad (22)$$

In the above equations \hbar is the Planck constant divided by 2π , ν is the vibrational frequency, and σ is the symmetry number of the rotation. L is the finite distance (of arbitrary large extension) along which the molecule of mass m is permitted to move. I is a 1D moment of inertia associated with the rotation axis defined in Equation 21 and I_1 , I_2 , I_3 are the three moments of inertia of a 3D rotor.

To obtain the vibrational frequencies of the various hindered rotational motions we tilted the given molecule around its equilibrium position. The rotations are performed by small angles around the x and y axis parallel to the soot surface and we calculated the energy in the tilted positions (but we did not optimized it). Then, the obtained energy values were fitted by a quadratic function:

$$E_{pot} = \frac{1}{2}k(x - x_0)^2 + a, \quad (23)$$

in which x denotes the tilt angle. The force constant k was then used for determining the frequency:

$$\nu = \frac{1}{2\pi} \sqrt{\frac{k}{I}}, \quad (24)$$

where I is the corresponding moment of inertia.

A similar procedure was repeated for the vibrational motion (i.e. hindered translational motion) along the z axis, but by replacing the moment of inertia by the mass of the admolecule in Equation 24.

The moment of inertia in the adsorbed phase was calculated around an axis perpendicular to the surface and passing through the center of mass of the admolecule. Note that this axis was considered as the z axis in our calculations.

The various constants corresponding to the different type of motions are collected in Table 3, and the partition functions calculated for the benzene molecule and the corresponding TS complex are given in Table 4. By using these values in Equation 18, we calculate that $\frac{k^{ads}}{k^{gas}} = 0.69$, indicating that the oxidation reaction of a benzene molecule by OH is slightly hindered when the molecule is adsorbed on a graphene sheet.

This result is not too surprising because the adsorption of the PAH on the graphene sheet prevents from the OH attack from one side of the PAH plane. Then, we expect from this simple argument that the rate constant should be more or less divided by a factor of two with respect to the reaction in gas

1
2
3 phase. Although this is a reductive reasoning, it gives some confidence on the
4 application of our SE-D model to reactivity problems. Note that our model
5 has been built to allow also the simulation of gas-surface processes on which
6 the surface can carry some defects like Stone-Wales defects[57], in plane and
7 edge atom vacancies[58]. Of course, the modification of the reactivity on a
8 defective surface is expected to be very different and non predictable a priori
9 with respect to the perfect surface analyzed here. But, in this latter case, the
10 conclusion is in accordance with the results of our energy optimization process,
11 (see above) which shows that the soot particle stabilizes the OH+benzene PRC
12 and the corresponding TS with respect to the gas phase situation.
13
14
15
16
17
18
19
20
21
22
23
24
25
26
27

28 **4 Conclusions**

29
30
31
32 In the present paper, we have used the AM1-D method to characterize the
33 oxidation by OH of a PAH molecule adsorbed on a soot surface modelled by
34 a graphene-like cluster. This method is based on an electrostatic and induc-
35 tion contribution calculated at the SCF AM1 level associated with a sum of
36 two-body dispersion terms of the $C^{(6)}/R^6$ form[37]. Indeed, the AM1-D is able
37 to properly describe the interactions between large aromatic systems, and it
38 can be used to study systems for which full *ab initio* calculations are prohib-
39 ited because of their large size. As a first application, we have detailed the
40 oxidation mechanism for benzene, which is the simplest aromatic molecule
41 (although not strictly a PAH molecule!). We have thus compared the charac-
42 teristics of the oxidation reaction for the adsorbed benzene with those of the
43 corresponding reaction in the gas phase. The main conclusion of the present
44 work is a clear inhibition of the oxidation process by the adsorption of the
45
46
47
48
49
50
51
52
53
54
55
56
57
58
59
60

1
2
3 benzene molecule on the soot surface. This conclusion is in qualitative agree-
4
5 ment with previous experimental observations, concerning, however, larger
6
7 PAH molecules[21]. For a better comparison with these experimental results,
8
9 further investigations devoted to naphthalene, phenanthrene and anthracene
10
11 molecules are under consideration. However, the corresponding calculations
12
13 are much more complex due to the presence of different non-equivalent car-
14
15 bon sites for the OH attachment in the oxidation mechanism. Moreover, the
16
17 real surface of soot is certainly not free of defects, and it would be thus also
18
19 important to characterize the oxidation reactions of PAH molecules adsorbed
20
21 on defective carbonaceous surfaces.
22
23

24
25 **acknowledgments** G.H.'s PhD is partly granted by the French Government
26
27 which is gratefully acknowledged.
28
29
30
31
32
33
34
35
36
37
38
39
40
41
42
43
44
45
46
47
48
49
50
51
52
53
54
55
56
57
58
59
60

References

- [1] B.J. Finlayson-Pitts, J.N. Pitt Jr. *Chemistry of the Upper and Lower Atmosphere: theory, experiments, and applications*. Academic Press : San Diego, 2000.
- [2] R.C. Pierce and M. Katz. *Dependency of polynuclear aromatic hydrocarbon content on size distribution of atmospheric aerosols*. Environ. Sci. Technol., 9 (1975) 347.
- [3] U. Pöschl, T. Letzel, C. Schauer, and R. Niessner. *Interaction of ozone and water vapor with spark discharge soot aerosol particles coated with benzo[a]pyrene: O₃ and H₂O adsorption, benzo[a]pyrene degradation, and atmospheric implications*. J. Phys. Chem. A, 105 (2001) 4029.
- [4] D.G. Aubin, J.P.D. Abbatt. *Laboratory Measurements of Thermodynamics of Adsorption of Small Aromatic Gases to n-Hexane Soot Surfaces*. Environ. Sci. Technol., 40 2006 179.
- [5] N.O.A. Kwamena, J.A. Thornton, J.P.D. Abbatt. *Kinetics of surface-bound benzo[a]pyrene and ozone on solid organic and salt aerosols*. J. Phys. Chem. A, 108 (2004) 11626.
- [6] N.O.A. Kwamena, M.E. Earp, C.J. Young, and J.P.D. Abbatt. *Kinetic and product yield study of the heterogeneous gas-surface reaction of anthracene and ozone*. J. Phys. Chem. A, 110 (2006) 3638.
- [7] N.O.A. Kwamena, M.G. Staikova, D.J. Donaldson, I.J. George, and J.P.D. Abbatt. *Role of the aerosol substrate in the heterogeneous ozonation reactions at the surface-bound PAHs*. J. Phys. Chem. A, 111 (2007) 11050.
- [8] R. Kotzick, U. Panne, and R. Niessner. *Changes in condensation properties of ultrafine carbon particles subjected to oxidation by ozone*. J. Aerosol. Sci., 28 (1997)

- 1
2
3 725.
4
5
6 [9] T. Novakov and C.E. Corrigan. *Cloud Condensation Nucleus Activity of the*
7 *Organic Component of Biomass Smoke Particles*. Geophys. Res. Lett., 23 (1996)
8 2141.
9
10
11
12 [10] C.N. Cruz and S.N. Pandis. *A study of the ability of pure secondary organic*
13 *aerosol to act as cloud condensation nuclei*. Atmos. Environ., 31 (1997) 2205.
14
15
16
17 [11] J.H. Seinfeld and S.N. Pandis. *Atmospheric Chemistry and Physics*. John Wiley
18 and Sons: New York, 1998.
19
20
21
22 [12] G.T. Wolf and R.L. Klimisch, Eds. *Particulate Carbon, atmospheric life cycle*.
23 Plenum Press: New York, 1982.
24
25
26
27 [13] E.D. Goldberg. *Black carbon in the environment: properties and distribution*. J.
28 Wiley: New York, 1985.
29
30
31
32 [14] J. Dachs and S.J. Eisenreich. *Adsorption onto aerosol soot carbon dominates*
33 *gas-particle partitioning of polycyclic aromatic hydrocarbons*. Environ. Sci.
34 Technol., 34 (2000) 3690.
35
36
37
38 [15] M.O. Andreae and A. Gelencser. *Black carbon or brown carbon ? The nature*
39 *of light-absorbing carbonaceous aerosols*. Atmos. Chem. Phys., 6 (2006) 3131.
40
41
42
43 [16] E.F. Mikhailov and S.S. Vlasenko. *Structure and optical properties of soot*
44 *aerosols in a moist atmosphere:2. Influence of hydrophilicity of particles on the*
45 *extinction, scattering, and absorption coefficients*. Atmos. Ocean. Phys., 43 (2007)
46 195.
47
48
49
50
51
52
53 [17] J.B. Renard, D. Daugeron, P. Personne, G. Legros, J. Baillargeat, E.
54 Hadamcik, J.C. Worms. *Optical properties of randomly distributed soot: Improved*
55 *polarimetric and intensity scattering functions*. Applied Optics, 44 (2005) 591.
56
57
58
59
60

- 1
2
3
4 [18] O.B. Popovicheva and A.M. Starik. *Aircraft-generated soot aerosols:*
5 *physicochemical properties and effect of emission into the atmosphere.* Atmos.
6 Ocean. Phys., 43 (2007) 147.
7
8
9
10 [19] D. Delhaye, PhD Thesis, Marseille, France (2007).
11
12
13 [20] R.L. Vander Wal, A.J. Tomasek. *Soot nanostructure: dependence upon synthesis*
14 *conditions.* Combustion and Flame, 136 (2004) 129.
15
16
17
18 [21] W. Esteve, H. Budzinski, and E. Villenave. *Relative rate constant for the*
19 *heterogeneous reactions of OH, NO₂ and NO radicals with polycyclic aromatic*
20 *hydrocarbons adsorbed on carbonaceous particles. Part 1: PAHs adsorbed on 1–2*
21 *µm calibrated graphite particles.* Atmos. Environ., 38 (2004) 6063.
22
23
24
25
26
27 [22] E. Perraudin, H. Budzinski, and E. Villenave. *Analysis of polycyclic aromatic*
28 *hydrocarbons adsorbed on particles of atmospheric interest using pressurized fluid*
29 *extraction.* Anal. Bioanal. Chem., 383 (2005) 122.
30
31
32
33 [23] P. J. DeMott, Y. Chen, S. M. Kreidenweis, L.M. McInnes, D.C. Rogers, D.E.
34 Sherman. *Ice Formation by Black Carbon Particles.* Geophys. Rev. Lett., 26 (1999)
35 2429.
36
37
38
39
40 [24] H. Saathoff, K.-H. Naumann, N. Riemer, S. Kamm, O. Möhler, U. Schurath, H.
41 Vogel, and B. Vogel. *The Loss of NO₂, HNO₃, NO₃/N₂O₅, and HO₂/HOONO₂*
42 *on Soot Aerosol: A Chamber and Modeling Study.* Geophys. Rev. Lett., 28 (2001)
43 1957.
44
45
46
47
48
49 [25] M. Wentzel, H. Gorzamski, K.-H. Naumann, H. Saathoff, S. Weinbruch.
50 *Transmission Electron Microscopy and Aerosol Dynamical Characterization of*
51 *Soot Aerosols.* J. Aerosol. Sci., 34 (2003) 1347.
52
53
54
55
56 [26] A. R. Chughtai, N. J. Miller, D. M. Smith, and J. R. Pitts. *Carbonaceous*
57 *Particle Hydration III.* J. Atmos. Chem., 34 (1999) 259.
58
59
60

- 1
2
3 [27] M. S. Munoz Salgado and M. Rossi. *Heterogeneous Reactions of HNO₃*
4 *with Flame Soot Generator under Different Combustion Conditions. Reaction*
5 *Mechanism and Kinetics.* Phys. Chem. Chem. Phys., 4 (2002) 5110.
6
7
8
9
10 [28] J.M.E Storey and J.F. Pankow. *Gas-particle partitioning of semi-volatile*
11 *organic compounds to model atmospheric particulate materialsI. Sorption to*
12 *graphite, sodium chloride, alumina, and silica particles under low humidity*
13 *conditions.* Atmos. Environ. A, 26 (1992) 435.
14
15
16
17
18
19 [29] K.U. Goss and S.J. Eisenreich. *Sorption of volatile organic compounds*
20 *to particles from a combustion source at different temperatures and relative*
21 *humidities.* Atmos. Environ., 31 (1997) 2827.
22
23
24
25
26 [30] B.T. Mader and J.F. Pankow. *Study of the Effects of Particle-Phase Carbon*
27 *on the Gas/Particle Partitioning of Semivolatile Organic Compounds in the*
28 *Atmosphere Using Controlled Field Experiments.* Environ. Sci. Technol., 36 (2002)
29 5218.
30
31
32
33
34
35 [31] B. Ngabé and L. Poissant. *Polycyclic Aromatic Hydrocarbons in the Air in the*
36 *St. Lawrence Basin (Québec).* Environ. Sci. Technol., 37 (2003) 2094.
37
38
39
40 [32] N.K. Lee, S. Park, and S.L. Kim. *Ab initio studies on the van der Waals*
41 *complexes of polycyclic aromatic hydrocarbons. I. Benzene naphthalene complex.*
42 *J. Chem. Phys., 116 (2002) 7902.*
43
44
45
46
47 [33] M.O. Sinnokrot, E.F. Valeev, and C.D. Sherrill. *Estimates of the Ab Initio Limit*
48 *for π - π Interactions: The Benzene Dimer.* J. Am. Chem. Soc., 124 (2002) 10887.
49
50
51
52 [34] C. Gonzales, T.C. Allison, and E.C. Lim. *Hartree-Fock Dispersion Probe of*
53 *the Equilibrium Structures of Small Microclusters of Benzene and Naphthalene:*
54 *Comparison with Second-Order Møller-Plesset Geometries.* J. Phys. Chem. A,
55 105 (2001) 10583.
56
57
58
59
60

- 1
2
3
4 [35] C. Gonzales and E.C. Lim. *Evaluation of the Hartree-Fock Dispersion (HFD)*
5 *Model as a Practical Tool for Probing Intermolecular Potentials of Small Aromatic*
6 *Clusters: Comparison of the HFD and MP2 Intermolecular Potentials.* J. Phys.
7 Chem. A, 107 (2003) 10105.
8
9
10
11
12 [36] J. Hepburn, G. Scoles, and R. Penco. *A simple but reliable method for the*
13 *prediction of intermolecular potentials.* Chem. Phys. Lett., 36 (1975) 451.
14
15
16 [37] B. Collignon, P.N.M. Hoang, S. Picaud, D. Liotard, M.T. Rayez, and J.C.
17 Rayez. *A semi-empirical potential model for calculating interactions between large*
18 *aromatic molecules and graphite surfaces.* J. Mol. Struct. Theochem, 772 (2006)
19 1.
20
21
22
23
24
25 [38] B. Collignon, PhD Thesis, Besançon, France (2006).
26
27
28 [39] M.I. Bernal-Uruchurtu, M.T.C. Martins-Costa, C. Millot, and M.F. Ruiz-López.
29 *Improving description of hydrogen bonds at the semiempirical level: water-water*
30 *interactions as test case.,* J. Comp. Chem., 21 (2000) 572.
31
32
33
34 [40] M.I. Bernal-Uruchurtu, M.F. Ruiz-López. *Basic ideas for the correction of*
35 *semiempirical methods describing H-bonded systems.,* Chem. Phys. Lett., 330
36 (2000) 118.
37
38
39
40
41 [41] W. Harb, M.I. Bernal-Uruchurtu, M.F. Ruiz-López. *An improved semiempirical*
42 *method for hydrated systems.,* Theor. Chem. Acc., 112 (2004) 204.
43
44
45 [42] J.P. McNamara and I.H. Hillier, *Semi-empirical molecular orbital methods*
46 *including dispersion corrections for the accurate predictions of the full range of*
47 *intermolecular interactions in biomolecules,* Phys. Chem. Chem. Phys., 9 (2007)
48 2362.
49
50
51
52
53
54 [43] S. Hamad, J.A. Mejias, S. Lago, S. Picaud, and P.N.M. Hoang. *A theoretical*
55 *study of the adsorption of water on a model soot surface. I. Quantum chemical*
56 *calculations.* J. Phys. Chem. B, 108 (2004) 5405.
57
58
59
60

- 1
2
3 [44] B. Collignon, P.N.M. Hoang, S. Picaud, and J.C. Rayez. *Clustering of water*
4 *molecules on model soot particles: an ab initio study.* Comp. Lett., 1 (2005) 277.
5
6
7
8 [45] B. Collignon, P.N.M. Hoang, S. Picaud, and J.C. Rayez. *Ab initio study of the*
9 *water adsorption on hydroxylated graphite surfaces.* Chem. Phys. Lett., 406 (2005)
10 430.
11
12
13
14 [46] G.C. Maitland, M. Rigby, E.R. Smith, W.A. Wakeham. *Intermolecular forces,*
15 *their origin and determination.* Oxford Science Publications, Oxford, 1987.
16
17
18 [47] S. Picaud, P.N.M. Hoang, S. Hamad, J.A. Mejias, and S. Lago. *A theoretical*
19 *study of the adsorption of water on a model soot surface. II. Molecular Dynamics*
20 *Simulations.* J. Phys. Chem. B, 108 (2004) 5410.
21
22
23
24
25
26 [48] T. Werder, J.H. Walther, R.L. Jaffe, T. Halicioglu, and P. Koumoutsakos. *On*
27 *the water-carbon interaction for use in molecular dynamics simulations of graphite*
28 *and carbon nanotubes.* J. Phys. Chem. B, 107 (2003) 1345.
29
30
31
32
33 [49] A. Alexiadis and S. Kassinos. *Molecular simulation of water in carbon nanotube.*
34 Chem. Rev., 108 (2008) 5014.
35
36
37
38 [50] I.W.M. Smith, A.R. Ravishankara. *Role of Hydrogen-Bonded Intermediates in*
39 *the Bimolecular Reactions of the Hydroxyl Radical.* J. Phys. Chem. A, 106 (2002)
40 4798.
41
42
43
44 [51] I.V. Tokmakov, M.C. Lin. *Kinetics and Mechanism of the OH + C₆H₆ Reaction:*
45 *A Detailed Analysis with First-Principles Calculations.* J. Phys. Chem. A, 106
46 (2002) 11309.
47
48
49
50
51 [52] S. Raoult, PhD Thesis, Université Bordeaux 1, France, 2003.
52
53
54 [53] S. Raoult, M.T. Rayez, J.C. Rayez, R. Lesclaux. *Gas phase oxidation of benzene:*
55 *Kinetics, thermochemistry and mechanism of initial steps.* Phys. Chem. Chem.
56 Phys, 6 (2004) 2245.
57
58
59
60

- 1
2
3
4
5
6
7
8
9
10
11
12
13
14
15
16
17
18
19
20
21
22
23
24
25
26
27
28
29
30
31
32
33
34
35
36
37
38
39
40
41
42
43
44
45
46
47
48
49
50
51
52
53
54
55
56
57
58
59
60
- [54] V.H. Uc, I. Garcia-Cruz, A. Hernandez-Laguna, A. Vivier-Bunge. *New Channels in the Reaction Mechanism of the Atmospheric Oxidation of Toluene*. J. Phys. Chem. A, 104 (2000) 7847.
- [55] M.J. Lundqvist, L.A. Eriksson. *Hydroxyl Radical Reactions with Phenol as a Model for Generation of Biologically Reactive Tyrosyl Radicals*. J. Phys. Chem, B. 104 (2000) 848.
- [56] R. Atkinson and R.J. Cvetanovic. *Activation energies of the addition of $O(^3P)$ atoms to Olefins*. J. Chem. Phys, 56 (1972) 432.
- [57] A. J. Stone and D. J. Wales. *Theoretical studies of icosahedral C_{60} and some related species*. Chem. Phys. Lett, 128 (1986) 501.
- [58] G.Ghigo, A. Maranzana, G. Tonachini, C.M. Zicovich-Wilson, M. Causa. *Modeling soot and its functionalization under atmospheric or combustion conditions by density functional theory within molecular (polycyclic-aromatic-hydrocarbon-like) and periodic methodologies*, J. Phys. Chem. B. 108 (2004) 3215.

1
2
3
4
5
6
7
8
9
10
11
12
13
14
15
16
17
18
19
20
21
22
23
24
25
26
27
28
29
30
31
32
33
34
35
36
37
38
39
40
41
42
43
44
45
46
47
48
49
50
51
52
53
54
55
56
57
58
59
60

Table 1

Selected parameters for the dispersion contribution to the SE-D potential calculated with the semi-empirical AM1 method. The parameters $C_C^{(6)}$, $C_H^{(6)}$, and $C_{OC}^{(6)}$ are given in $\text{kJ mol}^{-1} \text{ \AA}^6$; α is given in \AA^{-1} and R_0 in \AA .

	benzene
$C_C^{(6)}$	2207.94
$C_H^{(6)}$	48.6
$C_{OC}^{(6)}$	1923.51
α	3.96
R_0	2.68
α^{OH}	64.00
R_0^{OH}	2.75

Table 2

Comparison of the energy values and O–C distances obtained using the AM1 and AM1D methods. The energies are in kJ/mol while the distances in Å.

	PRC		TS		
	energy	d_{C-O}	energy	d_{C-O}	
AM1 gas phase ^a	-4.27	3.17	4.06	2.08	[a] AM1 calculations
AM1D gas phase	-12.1	2.81	1.26	2.09	
AM1D adsorbed phase	-13.9	2.81	-0.98	2.10	

lead to a gas phase TS energy slightly greater than zero i.e. TS lies above the reactants. The same is obtained when dispersion is included but with a much smaller magnitude. This result is proper to AM1 methodology applied to benzene molecule. Similar calculations on larger PAHs in the same conditions lead to small negative gas phase TS energies i.e. TS energy level is always below the energy of the reactants[38]. DFT and ab initio calculations on benzene and naphthalene show that the TS is also below the reactants, irrespective of the situation (gas-phase, with or without dispersion)[38,51,53]. This slight discrepancy between AM1 and more sophisticated methods in the case of benzene does not matter since benzene is considered here as a test molecule for our statistical approach explained further.

Table 3

Molecular constants corresponding to the different type of motions

		PAH(Benzene)	TS(Benzene + OH)
Gas phase	Translation	$M = 1.29 \cdot 10^{-25}$ kg	$M = 1.58 \cdot 10^{-25}$ kg
		$I_1 = 29.5 \cdot 10^{-46}$ kg m ²	$I_1 = 41.2 \cdot 10^{-46}$ kg m ²
	Rotation	$I_2 = 14.8 \cdot 10^{-46}$ kg m ²	$I_2 = 32.1 \cdot 10^{-46}$ kg m ²
		$I_3 = 14.8 \cdot 10^{-46}$ kg m ²	$I_3 = 20.8 \cdot 10^{-46}$ kg m ²
	$\sigma = 12$	$\sigma = 1$	
Adsorbed phase	Transl \rightarrow Vibr	$M = 1.29 \cdot 10^{-25}$ kg	$M = 1.58 \cdot 10^{-25}$ kg
		$\nu = 1.57 \cdot 10^{12}$ s ⁻¹	$\nu = 1.42 \cdot 10^{12}$ s ⁻¹
	Rot _x \rightarrow Vibr	$I_x = 14.8 \cdot 10^{-46}$ kg m ²	$I_x = 53.4 \cdot 10^{-46}$ kg m ²
		$\nu = 1.16 \cdot 10^{12}$ s ⁻¹	$\nu = 1.44 \cdot 10^{12}$ s ⁻¹
	Rot _y \rightarrow Vibr	$I_y = 14.8 \cdot 10^{-46}$ kg m ²	$I_y = 26.6 \cdot 10^{-46}$ kg m ²
		$\nu = 1.17 \cdot 10^{12}$ s ⁻¹	$\nu = 9.12 \cdot 10^{11}$ s ⁻¹
	Rotation _z	$I_z = 29.5 \cdot 10^{-46}$ kg m ²	$I_z = 37.5 \cdot 10^{-46}$ kg m ²
		$\sigma = 6$	$\sigma = 1$

Table 4

Molecular partition functions of the different type of motions

		PAH(Benzene)	TS(Benzene + OH)
Gas phase	Translation	$8.73 \cdot 10^{10} \cdot L \text{ m}^{-1}$	$9.63 \cdot 10^{10} \cdot L \text{ m}^{-1}$
	Rotation	$7.53 \cdot 10^3$	$1.87 \cdot 10^5$
Adsorbed phase	Transl \rightarrow Vibr	4.48	4.89
	Rot _x \rightarrow Vibr	5.85	4.84
	Rot _y \rightarrow Vibr	5.81	7.32
	Rotation _z	27.6	187

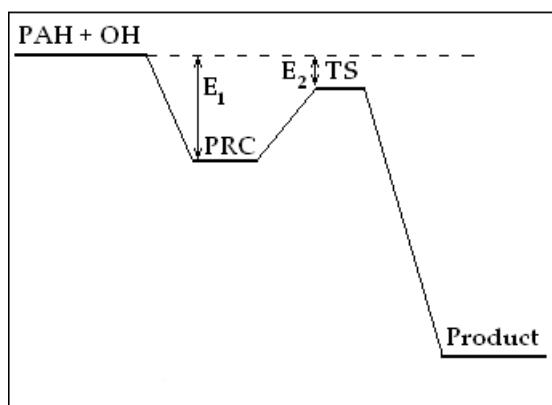


Fig. 1. Schematic representation of the oxidation reaction of PAH molecules by OH radical. The energy of the reactants (PAH + OH) is taken as the reference state for the definition of the energies. PRC and TS define the pre-reactive complex and the transition state, respectively.

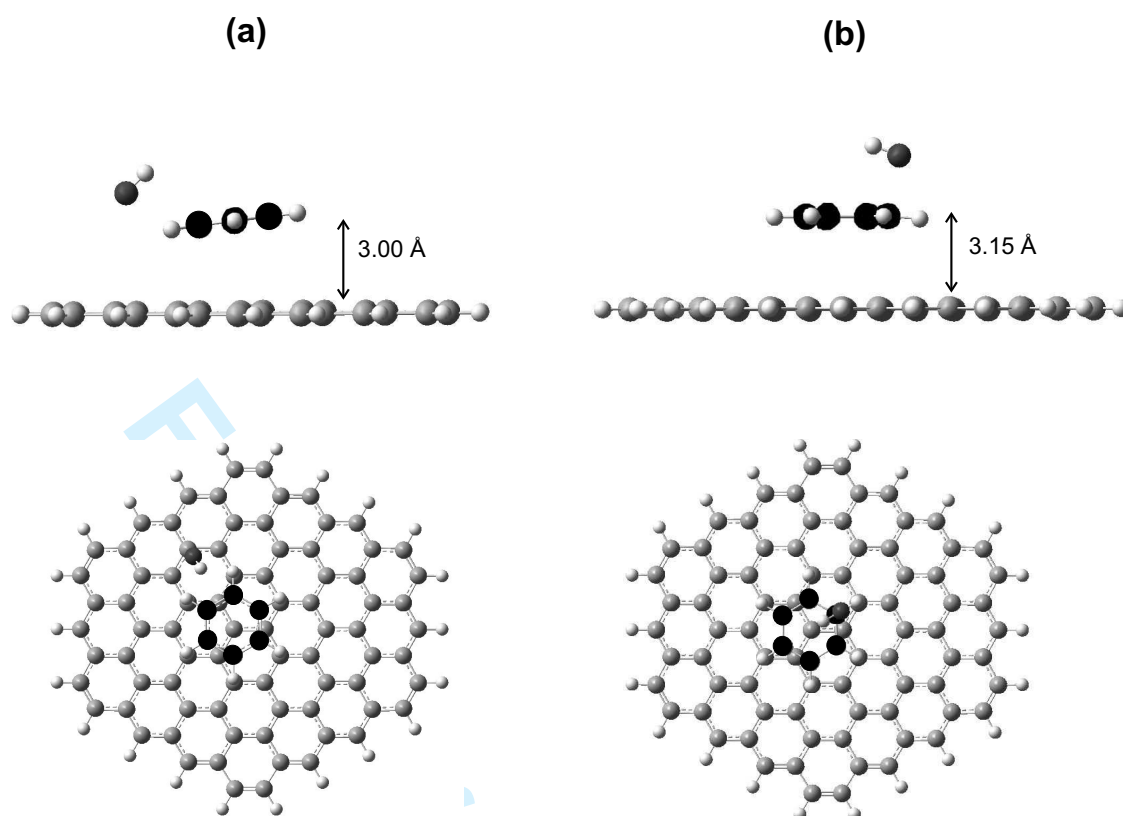


Fig. 2. Side (top of the figure) and top (bottom of the figure) views of the geometry of (a) the PRC and (b) the TS obtained for the oxidation reaction by OH of an adsorbed benzene molecule, using AM1-D method. The C atoms of the benzene molecule are represented as black circles for clarity, whereas the C atoms of the graphite cluster are represented as grey circles. Dark grey and white circles represent the O and H atoms, respectively. Note that the nearest C-C distances between the benzene molecule and the surface is also indicated on the side views.

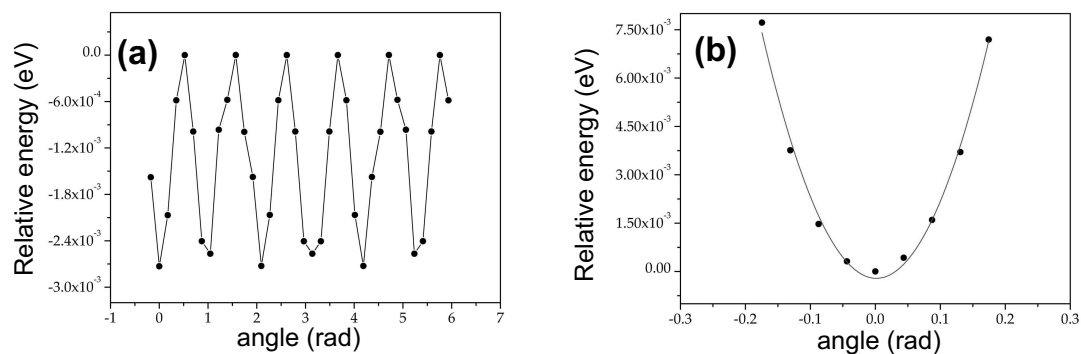
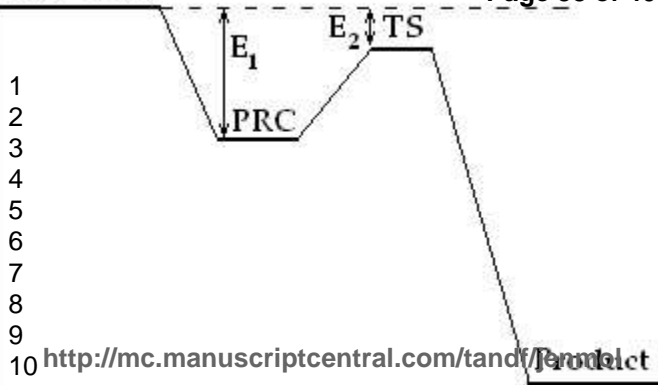


Fig. 3. Energy curves obtained upon rotating an adsorbed benzene molecule (a) around the z axis perpendicular to the surface of the $C_{80}H_{22}$ cluster and (b) around the x axis parallel to this surface. Note that the relative energy (in eV) is defined with respect to the maximum or the minimum of the energy curve. The angles are given in radian.



(a)

(b)

